Delft University of Technology
Faculty of Civil Engineering and Geosciences
Department of Design & Construction – Concrete Structures

Report nr. 25.5.12-02.

April 23, 2012

FEM analyses

Shear tests of Reinforced Concrete Slabs

Author:
Bc. Zdenka Procházková
Ir. E.O.L. Lantsoght
Dr. ir. C. van der Veen

Delft University of Technology
Faculty of Civil Engineering and Geosciences
Department of Design & Construction – Concrete Structures

Report nr. 25.5.12-02.

April 23, 2012

Shear tests of Reinforced Concrete Slabs
Experimental data of Undamaged Slabs
CONCEPT v. 29-07-2011

Author:
Bc. Zdenka Procházková
Ir. E.O.L. Lantsoght
Dr. ir. C. van der Veen

Delft University of Technology
Faculty of Civil Engineering and Geosciences
Department of Design & Construction – Concrete Structures
Stevinlaboratorium
Postbus 5048
2600 GA Delft
Telephone 015 2783990/4578
Telefax 015 2785895/7438

Contents

1. Introduction

The first goal of the FEM analysis for the Shear test of Reinforced Concrete Slab was to model the experiment close to the reality as much as possible. Then the influences of the changes in models e.g. changes in properties of concrete material, felt material, change of support conditions, etc. could be found and compared to the experimental data.

The second goal was to use the FEM analysis models to define effective width of the supports.

Four tests on slabs should be modeled: S1T1, S2T1, S3T1 and S8T1. All four slabs were loaded at the same position close to the simple support and in the middle of the width of the slab. The slabs differed in concrete compression and tensile strength, reinforcement ratio and boundary conditions.

In the chapter 2 the basic information of the experiment, dimensions of the specimens and measurement devices same for all four slabs were described. The FEM model of first slab S1T1 was considered as a basic model. The basic model was then adjusted according the description of slabs S2, S3 and S8. The basic model, results and effective width of S1T1 were described in a chapter 3. The models, results and effective widths of each slab were described in separate chapters 4, 5 and 6.

S1T1 was possible to successfully model within a given time. Models of other slabs S2T1, S3T1 and S8T1 would need further variation in models and additional test on felt. Although models of S2T1, S3T1 and S8T1 were not finished some conclusions could be made and effective widths in the linear stage could be found. The calculations of the steps of all models were fully converged until the peak load.

In a chapter 7 conclusions were presented and further research questions were suggested.

The nonlinear analysis software ATENA 3D version 4.2.7 and 4.3.0. have been used for the FEM analyses.

2. The description of the experiment

2.1. Test setup and specimen

Figure 1: Test setup

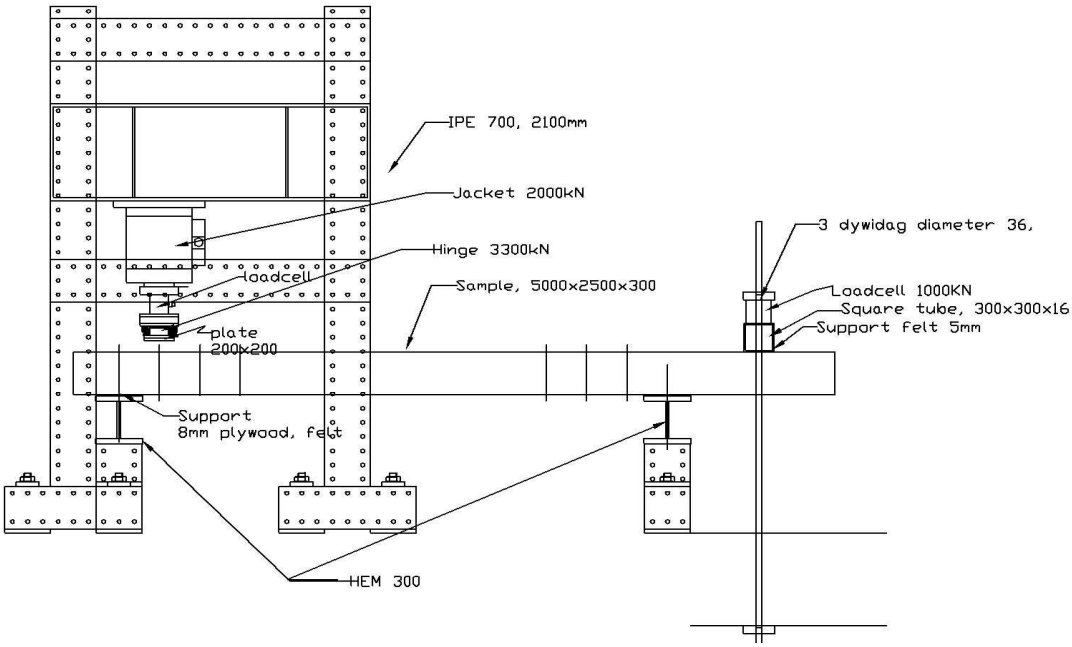

Figure 2: Test setup – side view

Slabs were supported by HEM steel beams. In order to avoid the stress concentration a layer of felt and plywood were placed between the steel beam and the slab. The heart of the plywood and felt coincided with the heart of the steel beam.

The slabs were prestressed to simulate continuous support. An external cables anchored to the floor of laboratory were used for prestressing (Figure 2).

The load was applied at the simple support (Figure 2), 600 mm from the heart of the steel beam support and in the middle of the width of the slab (a = 600mm, b_r = 1250mm;Figure 3 and Figure 4).

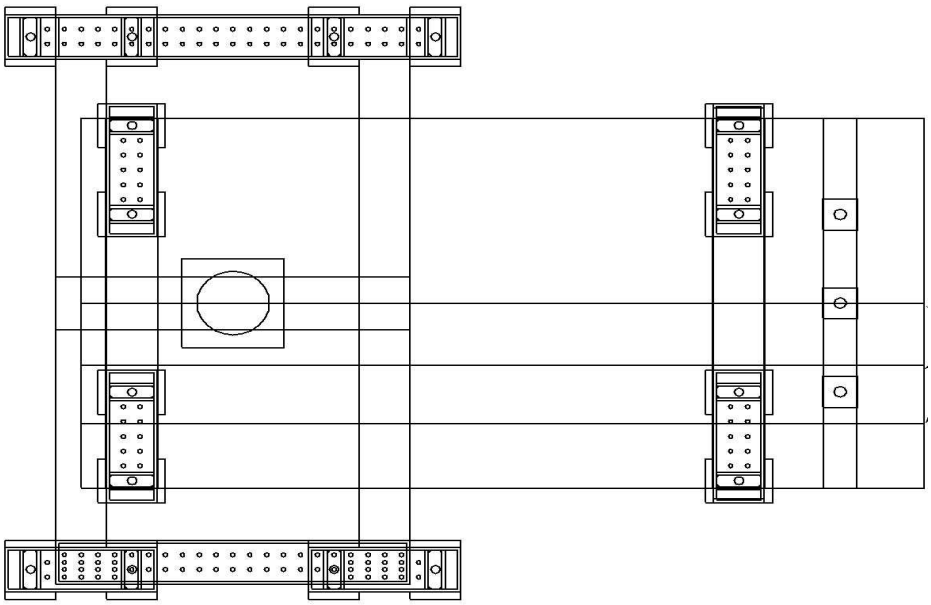

Figure 3: Test setup – to view

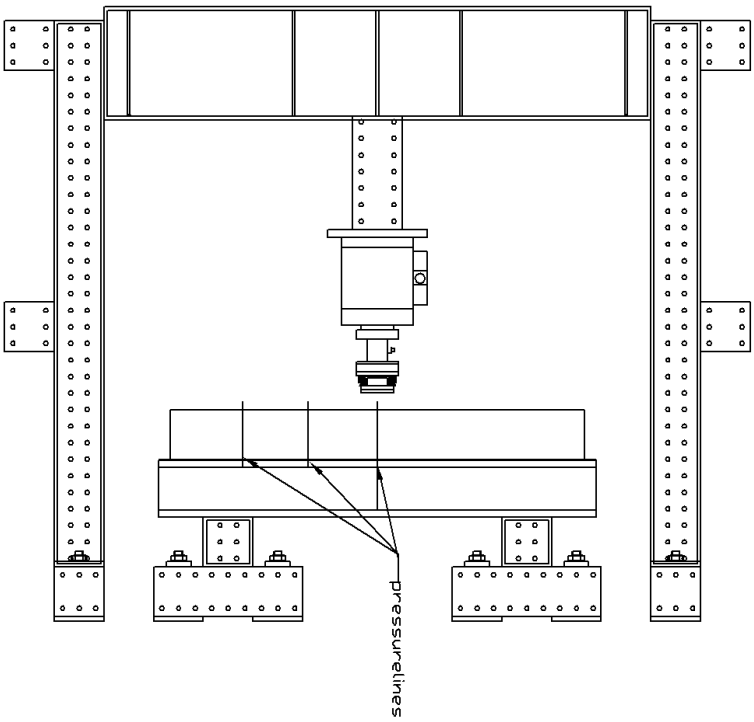

Figure 4: Test setup – front view

2.1.1. The basic variables of the specimens

Slabs had same dimensions – 5 meters long, 2.5 meters wide and 0.3 meters thick. All four slabs had same longitudinal reinforcement of ϕ20 – 125mm, in other word reinforcement ration ρ_l = 0,996%. The spacing of transversal reinforcement of ϕ10 was same for S1 and S2: spacing 250 mm (ρ_t = 0,132%) and same for S3 and S8: spacing 125 mm (ρ_t = 0,258%).

The concrete compressive and tensile strength properties were different for each slab. The variation of concrete properties and reinforcement are summarized in Table 1.

Table 1: Variation of the concrete properties and reinforcement of the concrete slabs

Slab	Concrete		Reinforcement	
	f_{cu} [MPa]	f_{tsplit} [MPa]	ρ_l [%]	ρ_t [%]
S1T1	38.18	3.54	0.996	0.132
S2T1	35.79	2.99	0.996	0.132
S3T1	52.10	4.22	0.996	0.258
S8T1	77.02	6.00	0.996	0.258

2.1.2. The variable of boundary conditions

The boundary conditions were different for each slab. The different sizes and thicknesses of loading plates were used and also two types of felt and different thickness of felt were applied on the steel beam supports. The variations of boundary condition are summarized in Table 2.

Size of the loading plate for S1T1 was 200x200 mm and because the hinge of the loading jack was of 200 mm diameter, the thickness of the loading plate was not important for FEM analysis.

For S2, S3 and S8 size of the loading plates was 300x300 mm and thicknesses of the loading plates can be seen in the Figure 5. The composition of loading plates for slab S2 and S3 was without extra plate. The Extra plate was used only in the test of slab S8.

In all experiments between steel beam support and concrete slab there was used same type and same thickness of plywood. Only the felt layer was different. For S1 new felt of type P50 and thickness 10 mm was used (Table 2). The same felt was used for testing of S2 and S3, therefore the state of the felt between steel beam support and concrete slab was considered as *used* felt. For S8 the felt type N100 and thickness of 15 mm was used.

Table 2: Variation of the boundary conditions

Slab	Felt			Loading plate	
	Type	Thickness [mm]	State	Size [mm]	Thickness [mm]
S1T1	P50	10	New	200x200	
S2T1	P50	10	Used	300x300	15 and 20
S3T1	P50	10	Used	300x300	15 and 20
S8T1	N100	15	Used	300x300	15, 20 and 25

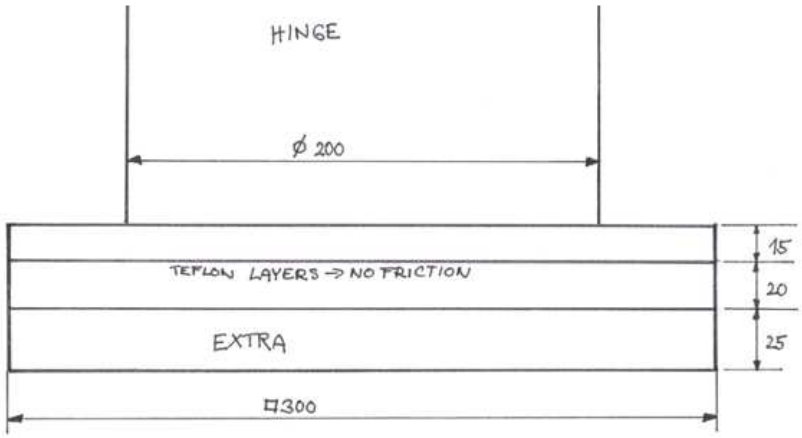

Figure 5: Composition of a loading plates for tests on slab S2, S3 and S8 (dimension in mm)

2.1.3. Position of Lasers

The displacement of the slab during experiment was measured by lasers. Layout of the lasers of the slab S1T1 can be seen in the Figure 6 and lay-out of the lasers for slab S2T1, S3T1 and S8T1 can be seen in the Figure 7.

For the FEM analyses four monitoring points were used to monitor the displacement of the slab. The positions of four lasers around loading plate were used. For S1T1 lasers number 4, 6, 8 and 10 were used (Figure 6) and for S2T1, S3T1 and S8T1 lasers number 14, 15, 16 and 17 were used (Figure 7).

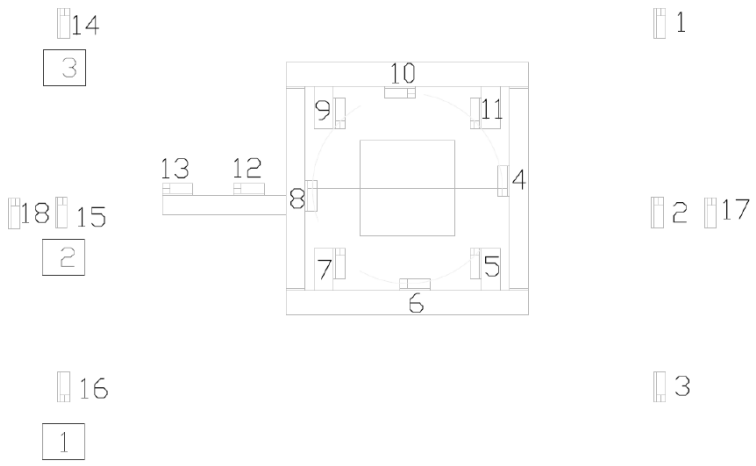

Figure 6: Lay-out of the lasers on S1

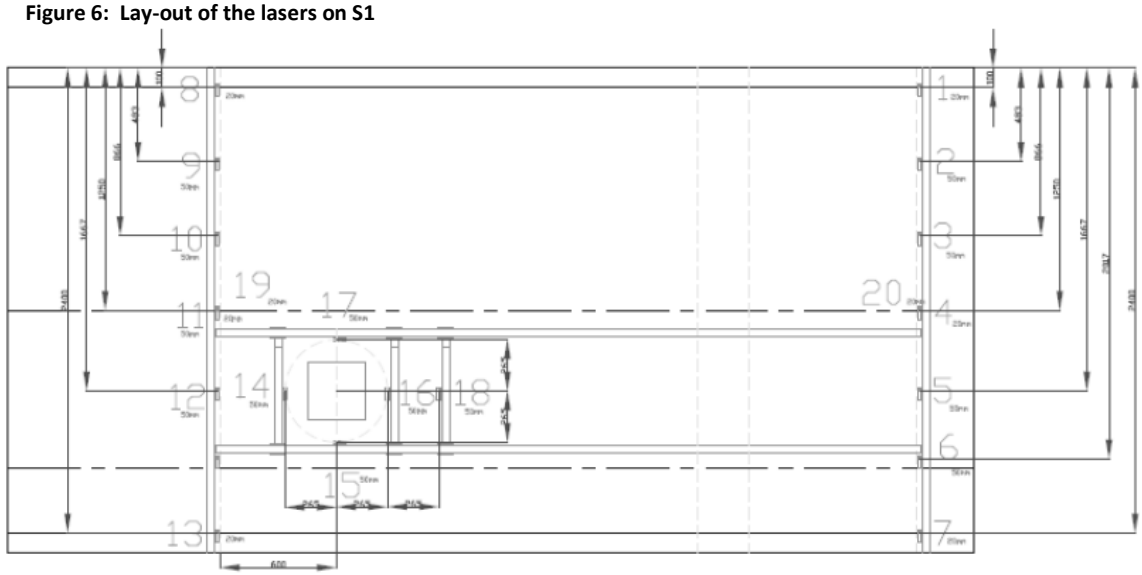

Figure 7: Lay-out of the lasers on S2, S3 and S8

2.2. Measured data

2.2.1. Load-displacement graphs

It was interesting to put all experimental results of S1T1, S2T1, S3T1 and S8T1 into one Load-Displacement diagram (Figure 8).

It could be seen that S1T1 and S2T1 had almost same stiffness response to the load but the peak loads were very different. The S1T1 had smaller loading plate but S2T1 had lower concrete compressive and tensile strength.

The L-D diagram of S3 and S8 showed stiffer response and larger peak load with respect to their higher concrete properties (Table 3).

Table 3: Variation of concrete properties and the reinforcement and peak loads measured in the experiment

Slab	Concrete		Reinforcement		Peak load
	f_{cu} [MPa]	f_{tsplit} [MPa]	ρ_l [%]	ρ_t [%]	[kN]
S1T1	38.18	3.54	0.996	0.132	954
S2T1	35.79	2.99	0.996	0.132	1374
S3T1	52.10	4.22	0.996	0.258	1371
S8T1	77.02	6.00	0.996	0.258	1481

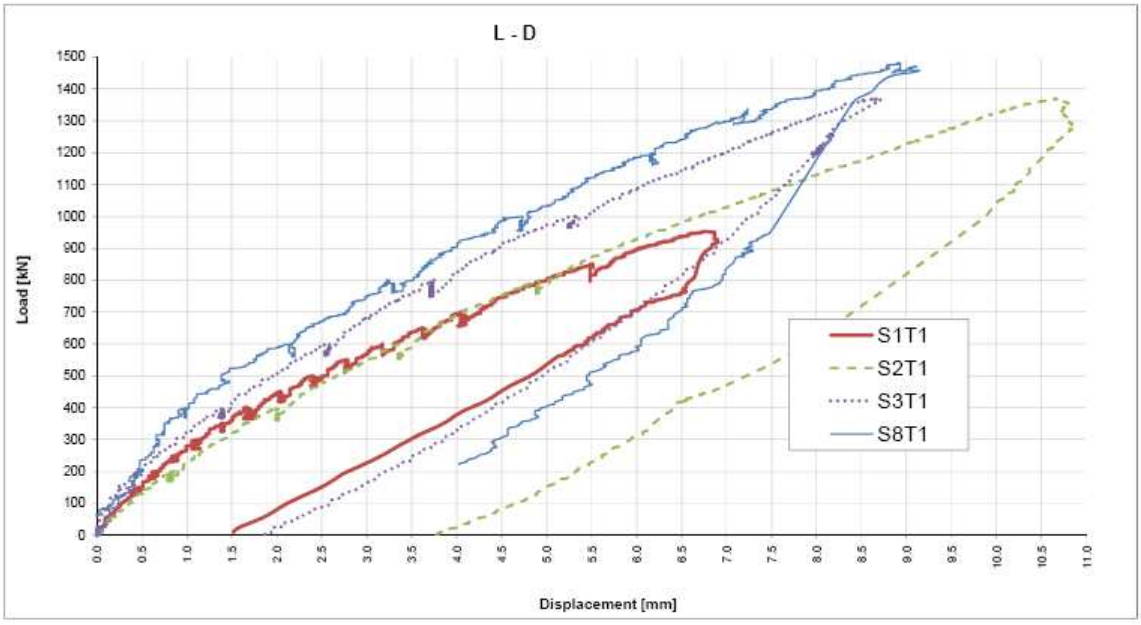

Figure 8: Results of S1T1, S2T1, S3T1 and S8T1 – Load-Displacement

3. S1T1

3.1. Basic model

The basic model consisted of 5 macroelements for concrete slab, 96 reinforcement bars, 1 loading plate, 3 prestressing cables, 1 beam for the prestressing cables, 1 beam which simulates floor where the prestressing cables are anchored, 2 surface springs, and 1 macroelement representing a layer of felt which was placed between slab and beam for prestressing cables.

The loading frame was not necessary to model. The HEM beam supports did not displace due to the loading during experiment and therefore the supports were not modeled and only surface springs were used to represent supports.

3.1.1. Geometrical model

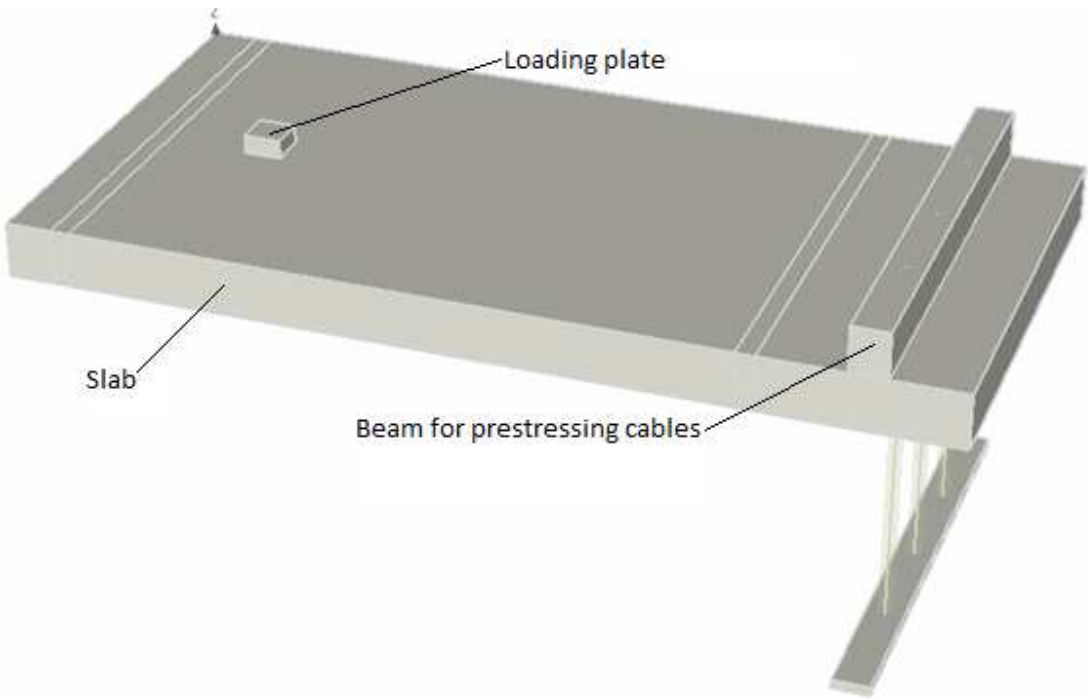

Figure 9: Model – top view

In the experiment the steel beam supports did not displace during loading, therefore supports were modelled as a surface springs with mechanical properties of felt and plywood which were placed between steel beam support and concrete slab. The mechanical properties of felt and plywood can be found in the section 3.1.2.3. and in the Figure 10 the surface springs can be seen. Although picture shows only one spring in the middle of the suport's surface, in FEM calculation springs were used in every node of surface element. The one spring only is the ATENA graphical representation of the surface springs.

In ATENA 3D it was not possible to create an independent surface on the surface of the macroelement. Therefore, in the model the concrete slab had to be divided into 5 macroelement with perfect contact properties. Two strips macroelements (Figure 9) had to be modeled in order that the surface springs could be placed on their bottom surfaces (Figure 10). In the fact this 5 macroelements behaved as a solid concrete slab.

In the experiment the size of the loading plate was same as the diameter of a hinge for the loading jack (200 mm), therefore in the geometrical model, the loading plate could be made as a 100 mm thick steel plate (see Figure 9).

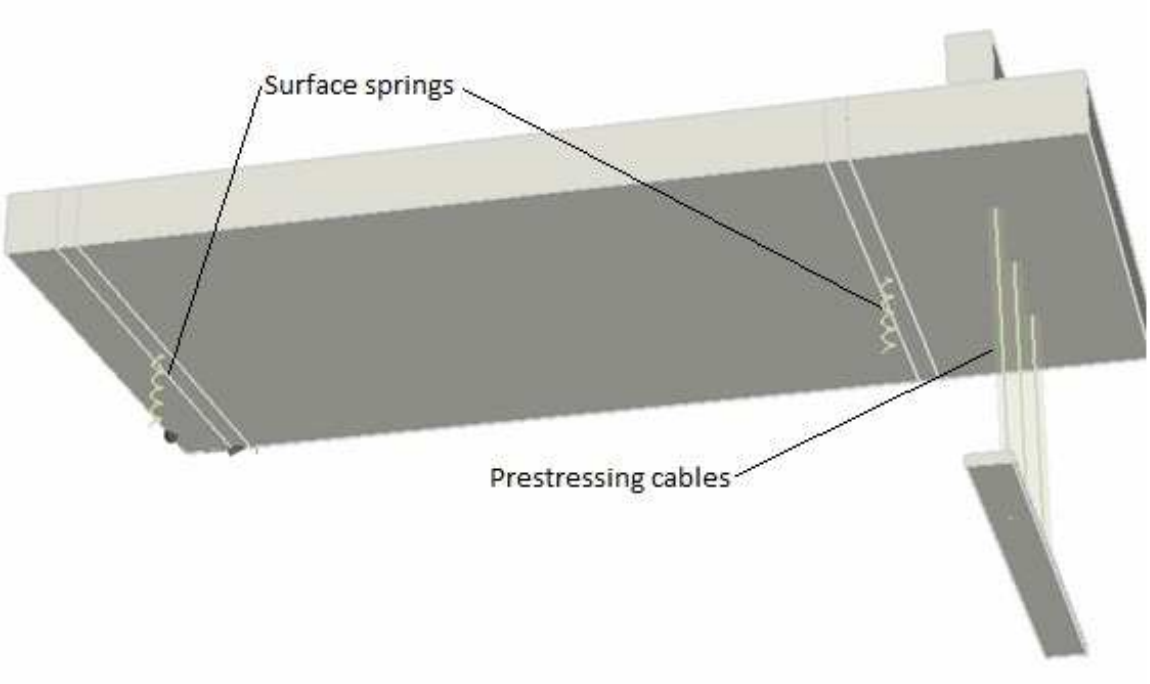

Figure 10: Model – bottom view

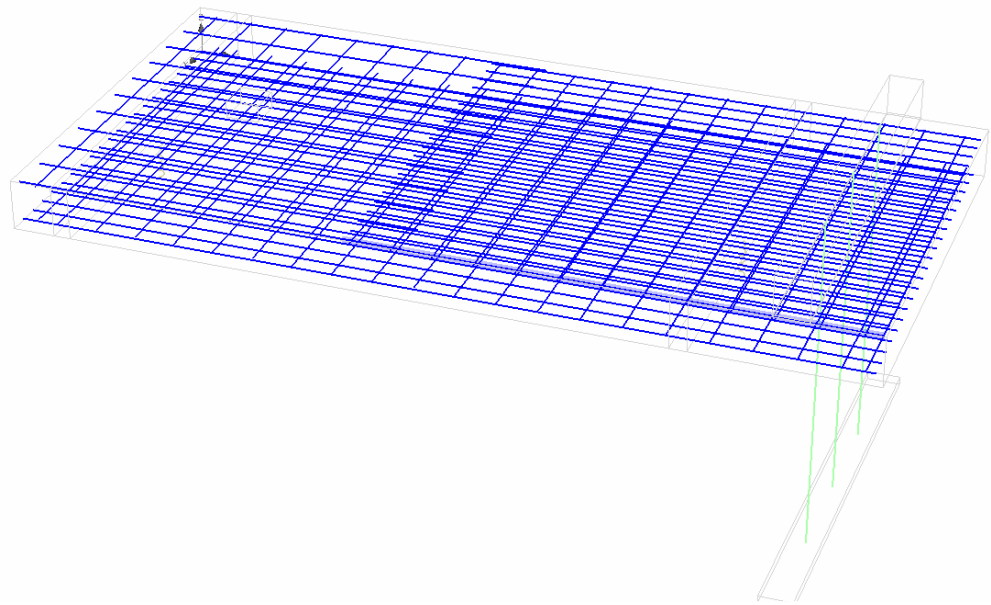

Figure 11: Model – reinforcement

The position of the longitudinal and transversal reinforcement can be seen in the Figure 11. For S1 and S2 the longitudinal reinforcement was of ϕ20 - 125mm (ρ_l = 0,996%) and the transversal reinforcement of ϕ10 - 250 mm (ρ_t = 0,132%). Modeling of reinforcement overlaps and hooks was not necessary.

3.1.2. Materials

3.1.2.1. Slab

The Material type CC3DNonLinCementitious2 was used for modeling of the concrete slab material. Mechanical properties are summarized in Table 4.

Table 4: Mechanical properties of the concrete slab

Properties		Value	Units
Elastic modulus	E	33420*	MPa
Poisson's ratio	μ	0.2**	-
Tensile strength	f_t	3.186***	MPa
Compressive strength	f_c	-32.45****	MPa
Specific fracture energy	G_f	6.803E-05**	MN/m
Crack spacing	s_{max}	Not activated	m
Tension stiffening	c_{ts}	Not activated	-
Critical compressive displacement	W_d	-0.0005**	m
Plastic strain at compressive strength	ε_{cp}	-9.711E-04**	-
Reduction of comp. strength due to cracks	$r_{c,lim}$	0.2**	-
Crack Shear Stiff. Factor	S_F	20**	-
Aggregate interlock MCF	Aggregate size	0.02*****	m
Fail. Surface excentricity		0.520**	-
Multiplier for the plastic flow dir.	β	0.000**	-
Specific material weight	ρ	0.023**	MN/m^3
Coefficient of thermal expansion	α	1.20E-05**	1/K
Fixed crack model coefficient		1**	-

* Calculated by ATENA, see CERVENKA, V., JENDELE, L., CERVENKA J. (2010)

** default value; see reference CERVENKA, V., JENDELE, L., CERVENKA J. (2010)

*** 0.9x3.54 MPa tensile strength based on splitting test, see reference LANTSOGHT, E.O.L. (2010) section 2.1.1)

**** 0.85x38.18 MPa compressive strength based on splitting test, see reference LANTSOGHT, E.O.L. (2010) section 2.1.1)

***** aggregate size rounded off 0.016 ~0.02

3.1.2.2. Felt

The Material type CC3DElastIsotropic was used for modeling the felt layer, which was placed on the concrete slab below the beam where the prestressing cables were fixed. This felt was same for all experiments. The mechanical properties are summarized in Table 5.

Table 5: Mechanical properties of the felt material

Properties		Value	Units
Elastic modulus	E	500*	MPa
Poisson's ratio	μ	0.0	-
Specific material weight	ρ	0.023**	MN/m^3
Coefficient of thermal expansion	α	1.20E-05**	1/K

* Based on Felt test – the stiffness of the specimens 32-35 after repeated loading and unloading was used (See PROCHAZKOVA, Z., LANTSOGHT, E.O.L. (2011))

** default value; see reference CERVENKA, V., JENDELE, L., CERVENKA J. (2010)

3.1.2.3. Surface springs

The Material type CCSpringMaterial was used for the modeling of the surface springs. The surface springs represented the combination of 8 mm of plywood and 10 mm of felt layer type P50 used between the concrete slab and the steel beam support. The stress-strain diagram, based on experimental data (PROCHAZKOVA, Z., LANTSOGHT, E.O.L. (2011), Test 35 was used) and which was used for the definition of spring properties, can be seen in the Figure 12. The first nonlinear part was taken according the Test 35 (also see Figure 13). The linear part up to stress of 28 MPa was used as a security that material did not fail in the calculation in the case of stress concentration which could occur during loading.

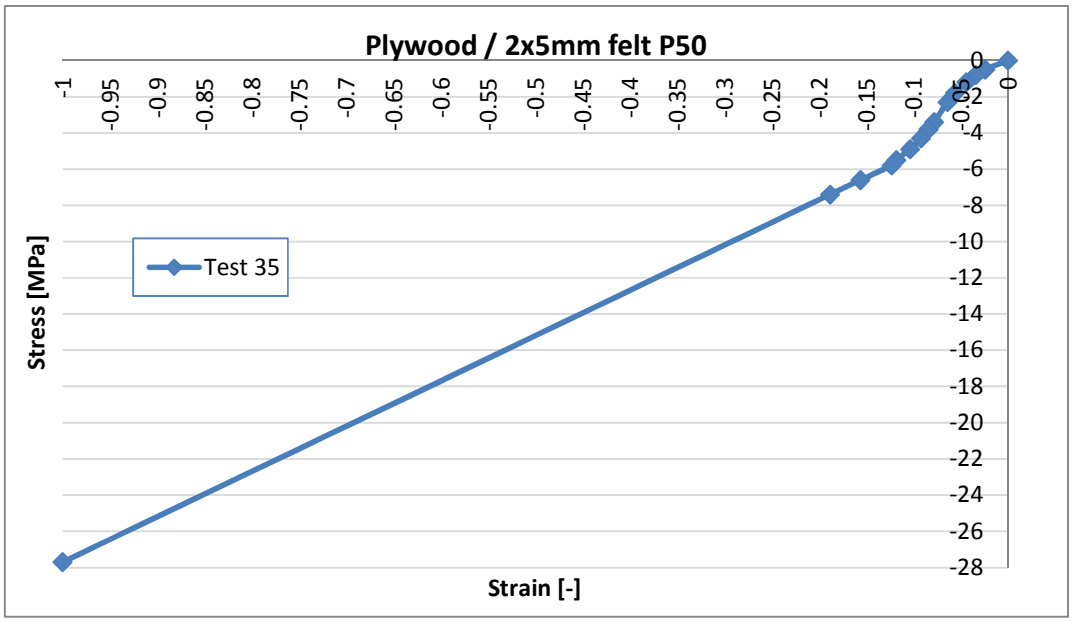

Figure 12: Stress-strain diagram of the surface spring properties – whole graph used in FEM model

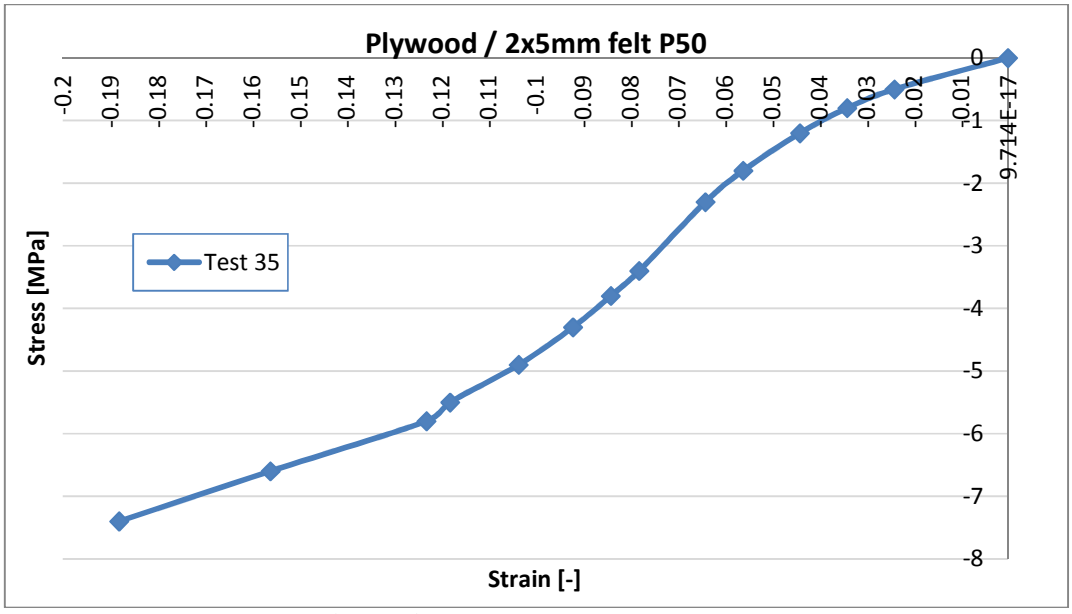

Figure 13: Stress-strain diagram of the surface spring properties – nonlinear part only

3.1.2.4. Supports and Loading plate

Material type CC3DElastIsotropic was used for the modeling of the supports and loading plate materials. The material for supports was also used for the elements – beam for prestressing bars and beam for the floor. The mechanical properties are summarized in Table 6.

Table 6: Mechanical properties of the supports and the loading plate

Properties		Value	Units
Elastic modulus	E	210*	GPa
Poisson's ratio	μ	0.3*	-
Specific material weight	ρ	0.023**	MN/m^3
Coefficient of thermal expansion	α	1.20E-05**	1/K

* Estimated value

** default value; see reference CERVENKA, V., JENDELE, L., CERVENKA J. (2010)

3.1.2.5. Cables

Material type CCReinforcement was used for the modeling of the prestressing cables. The mechanical properties are summarized in Table 7.

Table 7: Mechanical properties of the prestressing cables

Properties		Value	Units
Type	Bilinear		
Elastic modulus	E	200*	GPa
Yield strength	σ_y	1000	MPa
Specific material weight	ρ	7.850E-02**	MN/m^3
Coefficient of thermal expansion	α	1.228E-05**	1/K

* Estimated value

** default value; see reference CERVENKA, V., JENDELE, L., CERVENKA J. (2010)

3.1.2.6. Reinforcement D10 and D20

Material type CCReinforcement was used for modeling of reinforcement bars. The multilinear mechanical properties of reinforcement were used. The stress-strain diagram based on experiment performed by company Exova B.V. (see reference PROCHAZKOVA, Z., LANTSOGHT, E.O.L. (2011)) can be found in the Figure 14.

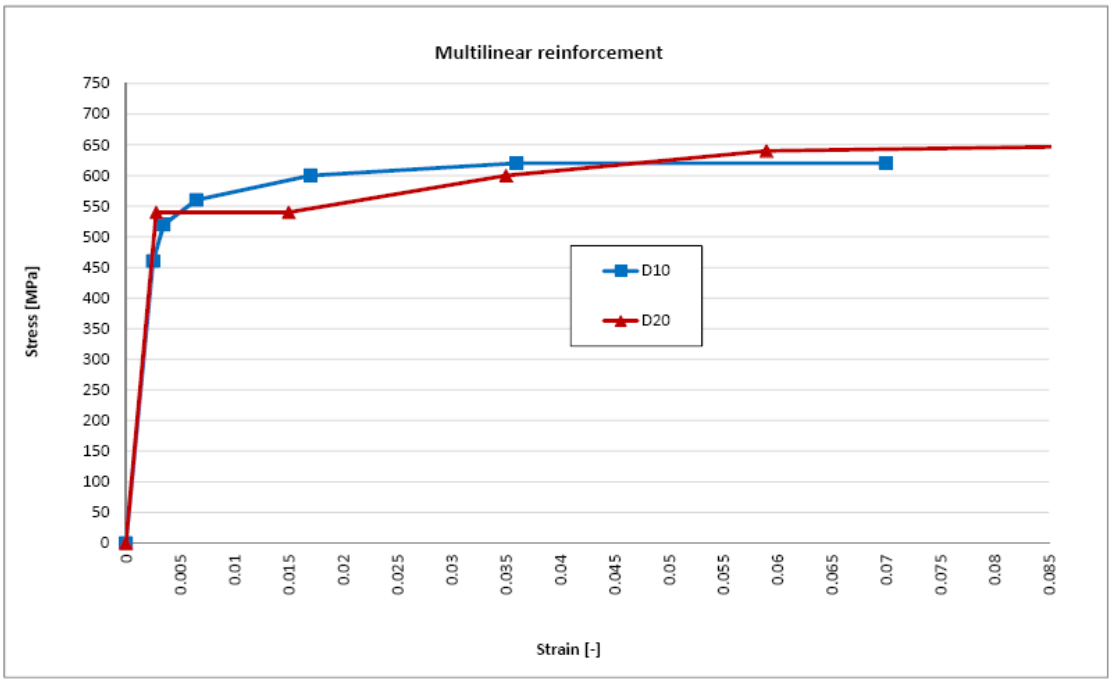

Figure 14: Stress-strain diagram of the reinforcement

3.1.3. Mesh

The brick elements were used for FEM mesh. Size of the mesh element was 100 x 100 and 50 mm height. That way was possible to achieve six elements over the height of the slab.

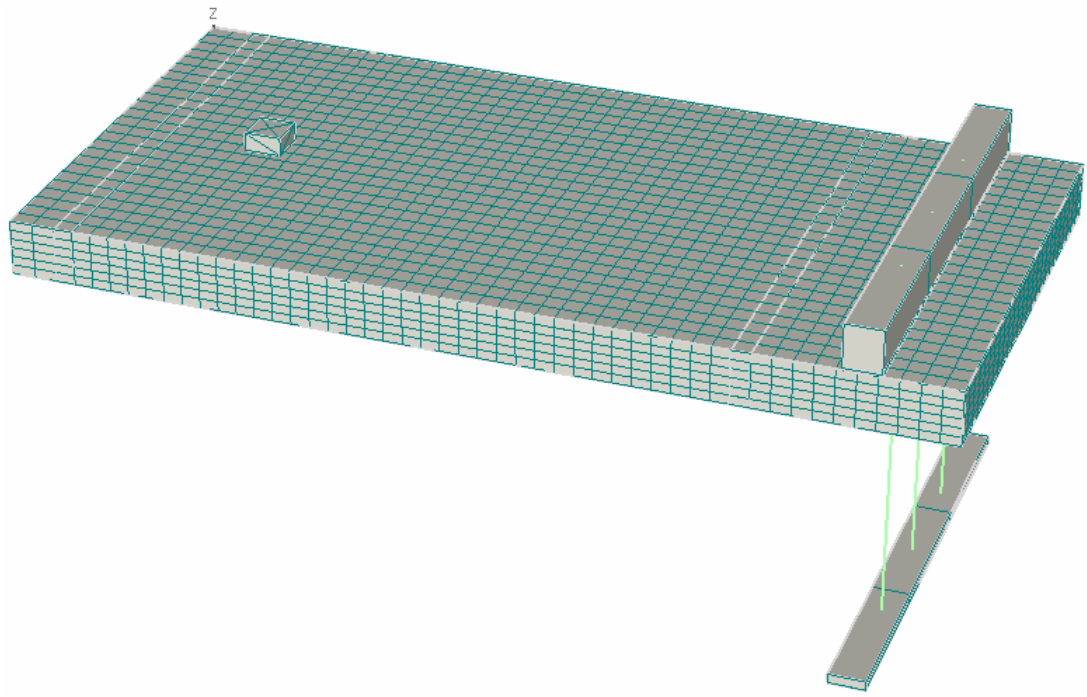

Figure 15: Mesh of the model

3.1.4. Monitoring points

In the experiment the displacement of the slab during loading was measured by lasers. The Figure 16 shows the lay-out of the lasers. In the model monitoring points were modeled at the same locations as laser number 4, 6, 8 and 10. See Figure 17 for the location of the monitoring points in the model.

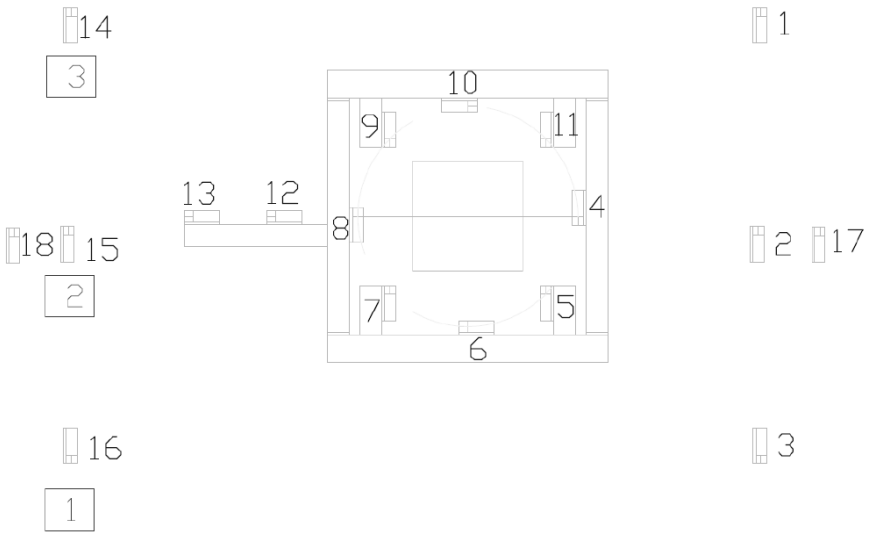

Figure 16: Lay-out of the lasers on slab S1T1 in the experiment (LANTSOGHT, E.O.L. (2010))

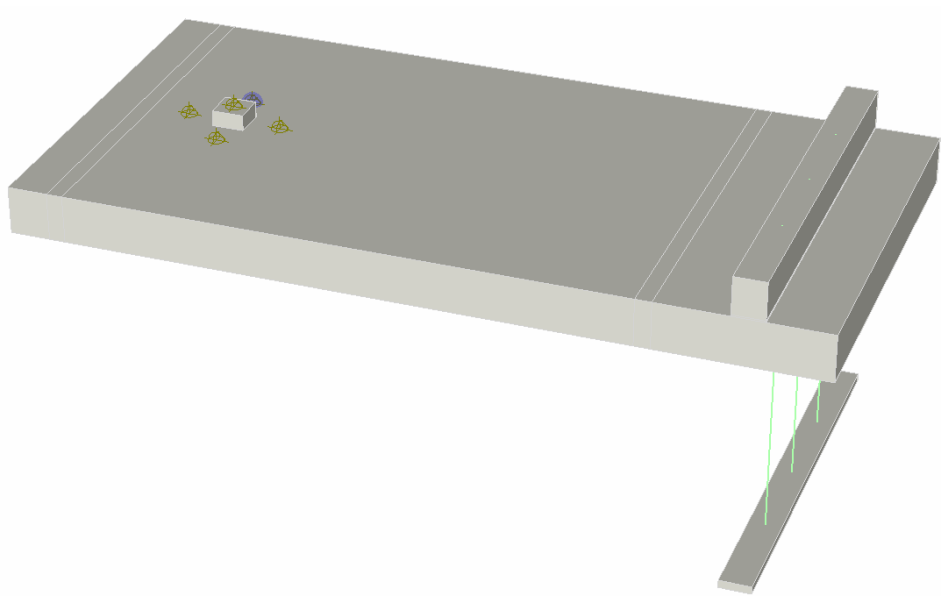

Figure 17: Location of the monitoring points in the model

3.1.5. Loading

There were four types of load cases applied: Supports – LC 3, Body force – LC 4, Temperature – LC 5 and Prescribed deformation – LC 2.

In the model the loading was exerted in order depicted in the Table 8.

Table 8: Load step – load case

Load step number	Load case type
1-10	Supports – LC 3, Body force – LC 4, Temperature – LC 5
11	Temperature – LC 5
>11	Prescribed deformation – LC 2 and Supports – LC 3

3.1.5.1. Supports - LC 3

The displacement of the slab in the z-direction was supported by the springs. The displacement in the y-direction was fixed by the Support load case on the line in the macroelement of felt (see Figure 18). Fixation in the x-direction was provided by the placing the Support load case to the point in the middle of the loading plate (see Figure 19).

The macroelement which represented the floor (and where prestressing cables were anchored) was fixed in all three directions on the bottom surface (see Figure 20).

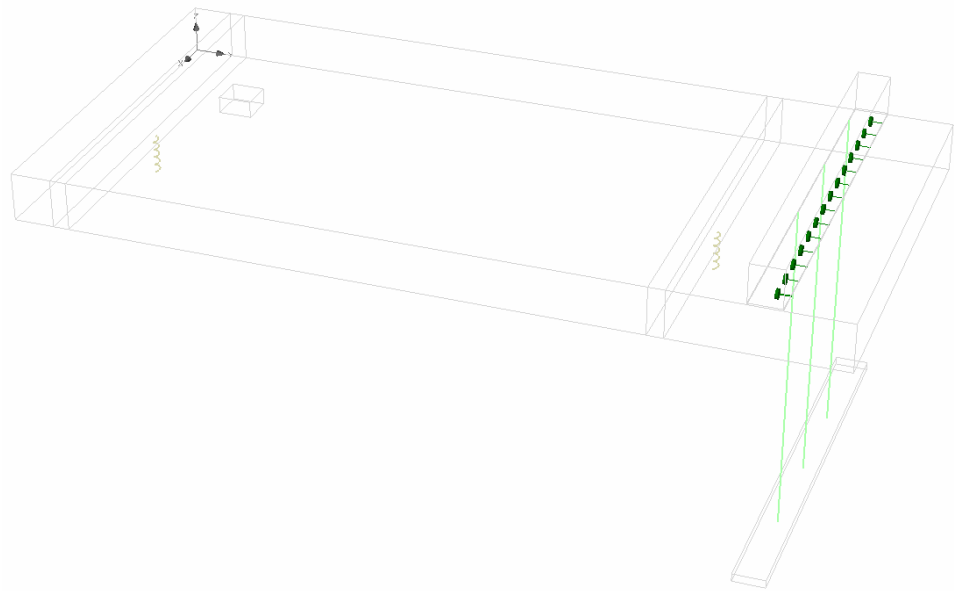

Figure 18: Fixation in the y-direction

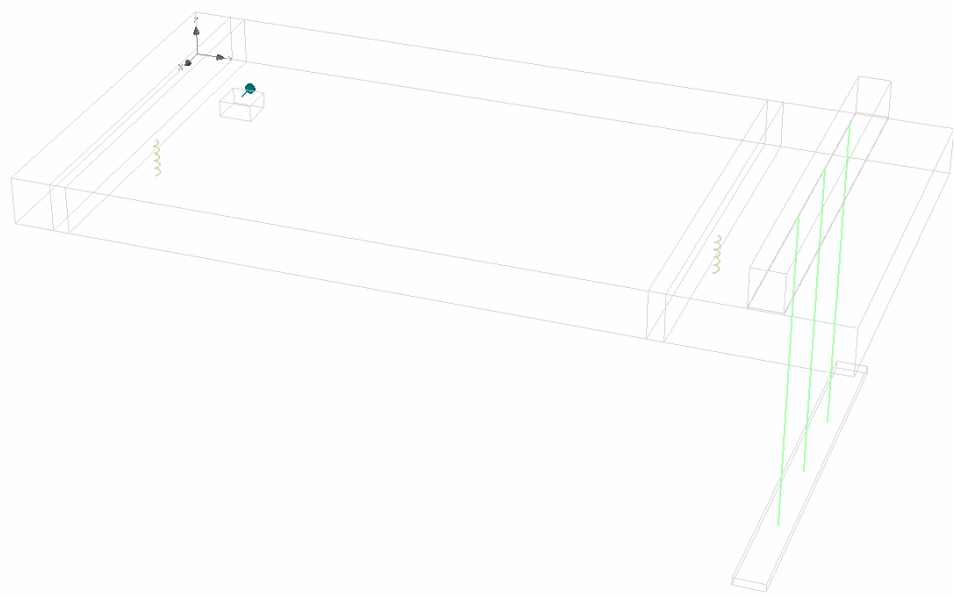

Figure 19: Fixation in the x-direction

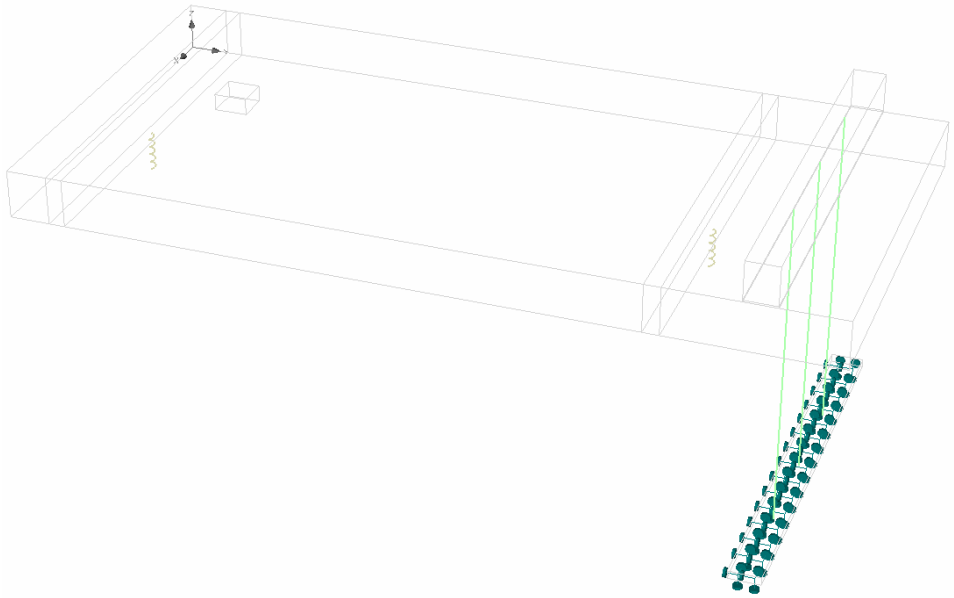

Figure 20: Fixation of the floor

3.1.5.2. Body force – LC 4

The load case Body force (self-weight) was employed to the 5 slab macroelements. The self-weight of all the other parts of the test setup were neglected. The Body force together with prestressing of cables was applied in the analysis in first ten steps (see Table 8).

3.1.5.3. Prestressing – LC5

In the experiment the cables were prestressed to the force of 15kN right before the loading of the slab. This prestressing was modeled by the load case Temperature applied on cables. Because the prestressing was applied in the analysis together with Body force the lower temperature (than could be analytically calculated) had to be used. This temperature differentiated with the variation of the felt type (see Table 9).

Table 9: The variation of the temperature used for prestressing of cables

Type of felt	**Temperature**
P50 – new	-22 K
P50 – used	-17 K
N100 – 15 mm - used	-20 K

3.1.5.4. Prescribed deformation - LC2

The load on the slab was modeled by load case Prescribed deformation. Unit displacement (for one step) was set to -0.0001 m in the z-direction. The Multiplication factor to the unit displacement was used to reduce the prescribed displacement to let analysis completely converge in the critical loads e.g. where a lot of cracks occur or at the peak load.

3.1.6. Analysis

Solution parameters used in the analysis are described in the Table 10.

Table 10: Solution parameters

General		
Solution method	Newton-Raphson*	
Optimize node numbers	Sloan*	
Update stiffness	Each iteration*	
Stiffness type	Tangent*	
Iteration limit for one analysis step	40 and 80**	
Displacement error tolerance	0.01 [-]*	
Residual error tolerance	0.01 [-]*	
Absolute residual error tolerance	0.01 [-]*	
Energy error tolerance	0.0001 [-]*	
Line Search		
Solution method	With iterations*	
Unbalanced energy limit	0.8 [-]*	
Limit of line search iterations	2*	
Line search limit - min	0.01 [-]*	
Line search limit - max	1 [-]*	
Condition break criteria	Break immediately [-]	Break after step [-]
Displacement error multiple	10000*	1000*
Residual error multiple	10000*	1000*
Abs. residual error multiple	10000*	1000*
Energy error multiple	1000000*	10000*

*default value; see reference CERVENKA, V., JENDELE, L., CERVENKA J. (2010)

** 40 iterations were used steps 1-11, in the rest of the steps 80 iterations were used

3.2. Results

The maximum load measured during experiment S1T1 was 954 kN. In the FEM analyses the maximum peak loads were in the range 852 – 923kN. In the percentage the difference of the results from the experiment and models was about 3.4 – 11 %. The best model (presented in the Figure 21) had the peak load of 882 kN. It can be considered that the results were quite good. The calculations of the steps of all models were fully converged until the peak load.

The crack pattern, however, did not correspond to the experimental observations. The crack pattern in the experiment showed one crack at the front face of the slab and in the FEM models two cracks at the front face had appeared (Figure 22). The distribution of cracks might be highly influenced by the size and position of the mesh elements. The summation of widths of cracks at the front face of the slab in the FEM models was close to the width of crack measured in experiment. The crack widths of FEM model were 2.1 mm and there was measured width of 1.8 mm in the experiment.

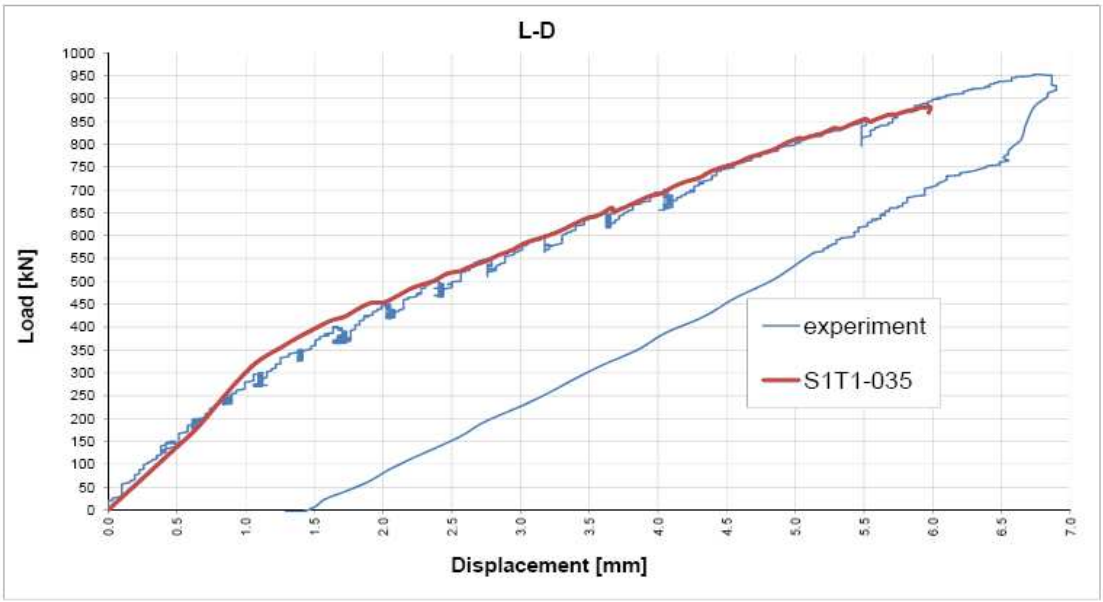

Figure 21: S1T1 load-displacement graph of the best model

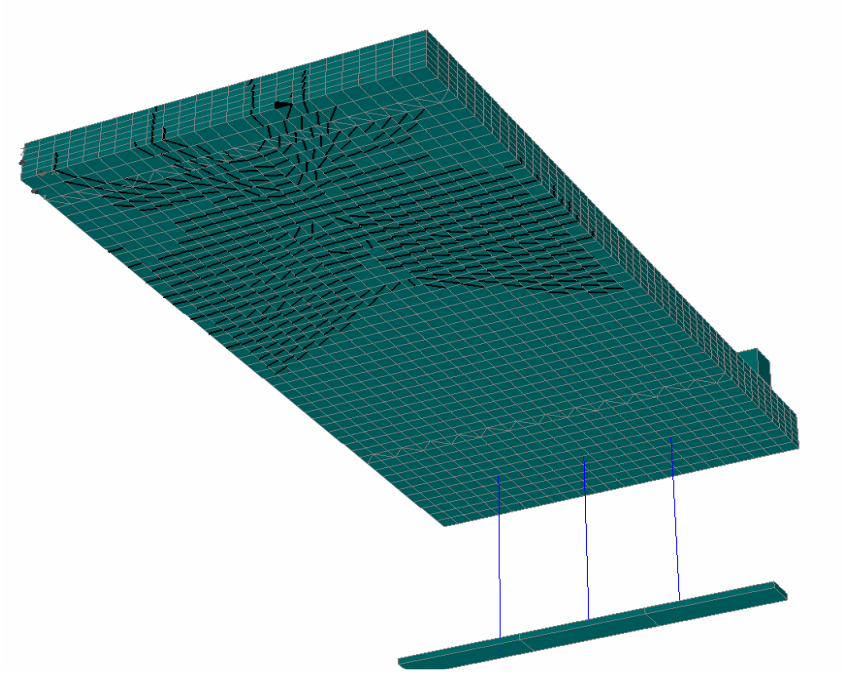

Figure 22: S1T1 crack pattern – two cracks at front face, width 2.1 mm

3.3. Effective width

The supports in the FEM model were modeled by surface springs. The surface spring contained 52 nodes, which gave 26 nodes for each edge of the surface. For each node the value of the stress could be found and the effective width for different loads was determined. The effective widths at different loads are presented in the Table 11.

The crack visualization was filtered to the minimum crack width 0.0001 meters. In the model of S1T1 the first cracks of the size 0.0001 meters started to appear under the load of 423 kN and effective width at that load was 2.06 m (the width of the slab and length of the surface support was 2.5 meters). At the peak load the effective width was limited to 1.4 meters.

Table 11: S1T1 effective width

S1T1			
Load [kN]	step	Cracks 0.0001 m	Effective Width [m]
48	20	No	2.4916
107	25	No	2.4565
147	28	No	2.4458
190	31	No	2.3515
318	35	No	2.3376
401	40	No	2.1240
423	42	2	2.0656
439	43	around 5	2.0443
502	49		1.7807
601	58		1.6001
708	72		1.5435
880	130		1.4114
882	134		1.4090

4. S2T1

4.1. Model description

Slab S2 was same as slab S1 only differences were in mechanical properties of concrete and in the boundary conditions – different felt and plywood properties and larger loading plate. The variations of models are described in the following sections.

4.1.1. Concrete

S1 and S2 were casted from same composition of concrete - Cast 1. Slab S1 was tested at the concrete age of 28 days and slab S2 was tested at the concrete age of 65 days. Concrete compressive strength was based on the cube test and tensile strength on tensile splitting test of cube specimens casted from the same composition of the concrete and tested at the same age as the corresponding concrete slabs (see reference LANTSOGHT, E.O.L., 2010). Although S2 was tested at older age of the concrete, the cube and splitting tests showed lower compressive and tensile strength of the concrete (see Table 1).

In FEM model of S2T1 the same mechanical properties of the concrete as in the model of S1T1 were used (see Table 4), only compressive and tensile strengths were changed according the results on cube specimens. The concrete compressive strength for S2T1 was 35.79 MPa and the tensile strength was 2.99 MPa.

4.1.2. Felt

Additional compression tests on felt and plywood showed that their mechanical properties had changed under the cyclic loading (see reference PROCHAZKOVA, Z., LANTSOGHT, E.O.L. (2011)). Test S1T1 was performed with use of a completely new felt. After the tests on slab S1, the felt between the steel beam support and the concrete slab remained and slab S2 was tested on that same felt and plywood layer. Therefore for FEM model it was assumed that the properties of felt and plywood should be modeled based on results from repeated loading. The second loading line of test 32 from the Figure 23 was used to model *used* felt and plywood. But results showed that model with *new* felt and plywood properties (same as in model of S1T1; see Figure 13) was closer to the experimental results than the model with used felt and plywood layer properties.

The difference in the models with *new* and *used* felt and plywood layer can be seen in a Figure 24. The model S2T1-002 was with *used* felt and plywood properties and the model S2T1-013 was with *new* felt and plywood properties.

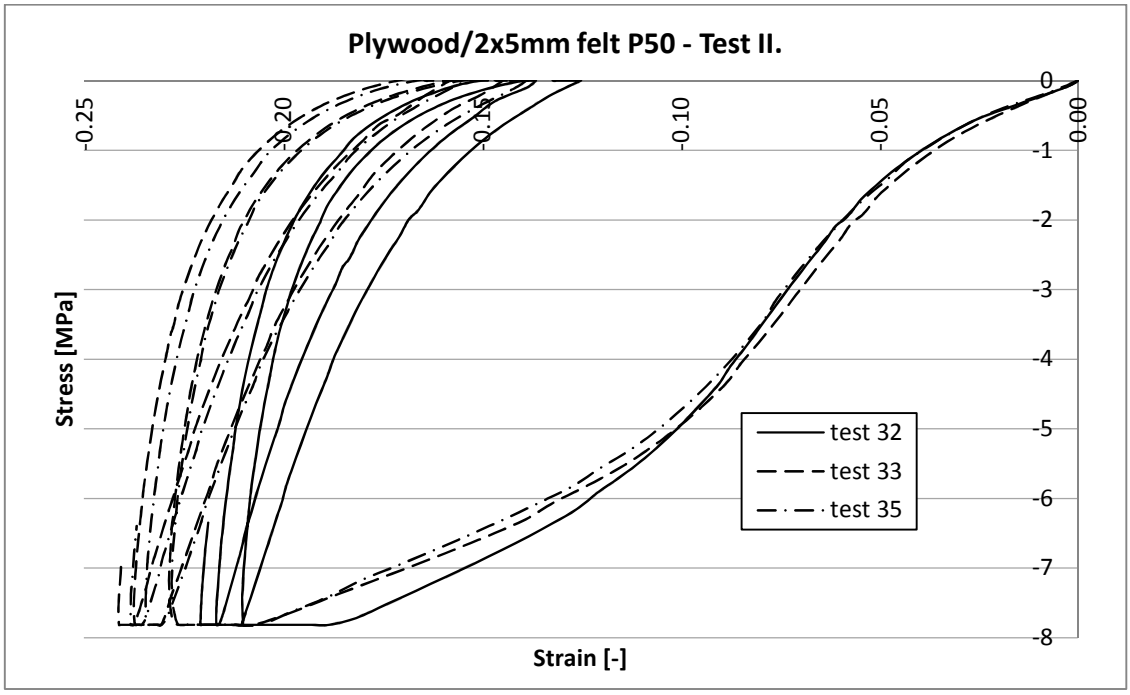

Figure 23: Felt and plywood properties taken from reference PROCHAZKOVA, Z., LANTSOGHT, E.O.L. (2011)

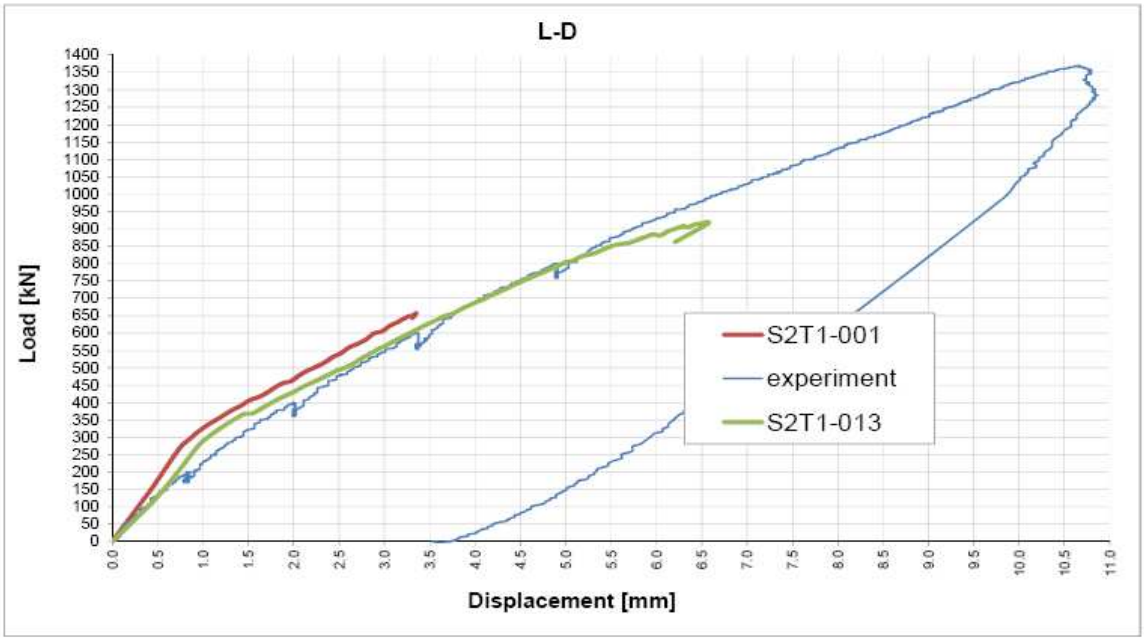

Figure 24: S2T1-002 with *used* felt and S2T1-013 with *new* felt (same as S1T1)

4.1.3. Loading plate

The loading plate for tests on slab S1 was of the size 200x200 mm. The loading plate for test on S2 was 300x300 mm size. First it was assumed that the loading plate of S2T1 could be modeled in the same way as in the model of S1T1. It was 100 mm thick loading plate like depicted in the Figure 25 and Figure 26. This model S2T1-006 was showing very poor results and slab was failing under the half of the load (682 kN) then the maximum load (1374 kN) measured in the experiment. In the model with thick loading plate the slab was failing due to the crashing of the concrete around the corners of the loading plate.

Therefore model S2T1-008 was made with loading plate composed from 12-sided polyhedron of 200 mm diameter corresponding to the diameter of the hinge for the loading jack and 15 mm thin steel loading plate of the 300x300 mm size (Figure 27 and Figure 28). This model reached peak load of 942 kN. The loading plate was not modeled according the actual loading plate as in the experiment yet, but results showed that the performance of a slab could be dependent on the thickness of the loading plate and ratio between the size of the loading plate and the diameter of the hinge.

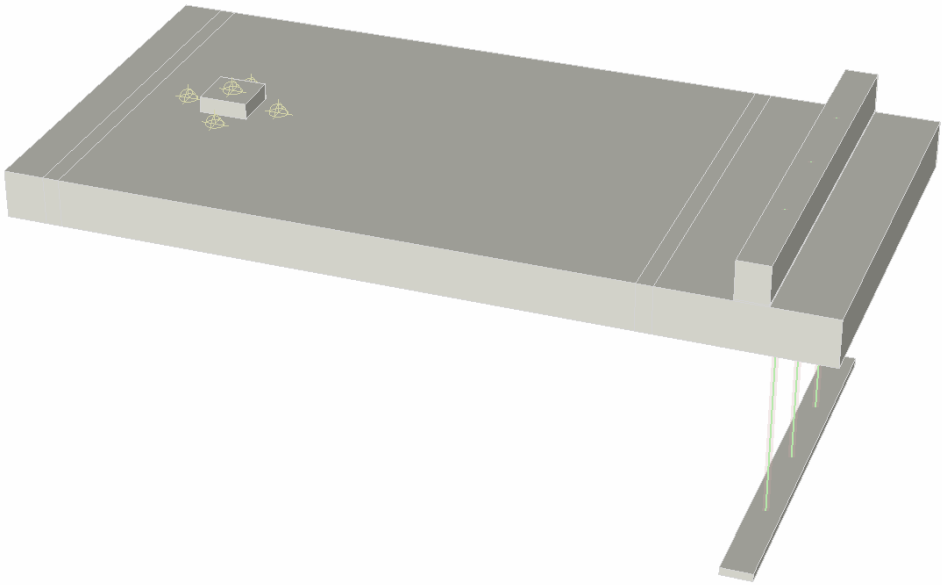

Figure 25: S2T1-006 model with 100 mm thick loading plate

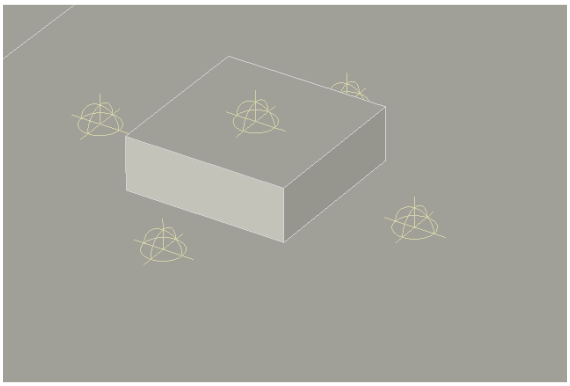

Figure 26: S2T1-006 model with 100 mm thick loading plate - detail

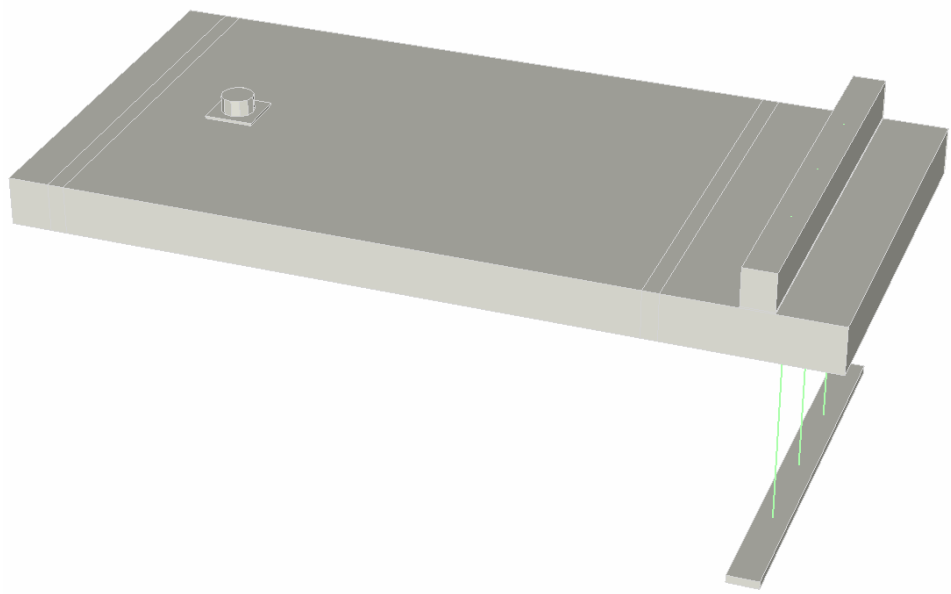

Figure 27: S2T1-008 model with 15 mm loading plate of the size 300x300 and hinge of 200 mm diameter

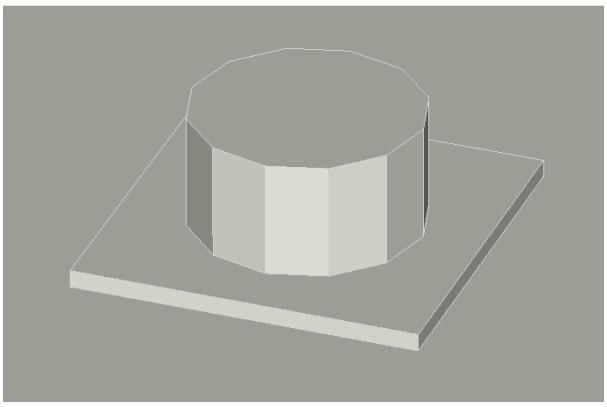

Figure 28: S2T1-008 with 15 mm loading plate of the size 300x300 and loading jack of 200 mm diameter -detail

The loading plate's composition according the experiment for slabs S2, S3 and S8 are depicted in the Figure 29 and Table 12. For slab S2 the loading plate composition consisted of two steel plates of thickness 15 and 20 mm with greasy Teflon layer (zero friction) in between steel plates and the hinge for the loading jack of 200 mm diameter (Figure 29).

The loading plate of the model S2T1-013 was modeled according the composition of the loading plate in the experiment (Figure 30 and Figure 31). The properties of the Teflon layer in the FEM models are summarized in Table 13. The material 3D Interface was used and for the first models with Teflon layer default values for normal and tangential stiffness were left, only friction coefficient and cohesion values were changed to zero.

The better definition of Teflon layer might be done to make FEM model closer to the reality but it would require more time investment, which was not available. The model S2T1-013 showed best results and despite of the fact that Teflon layer was not properly defined it still showed better results than the model with thick loading plate.

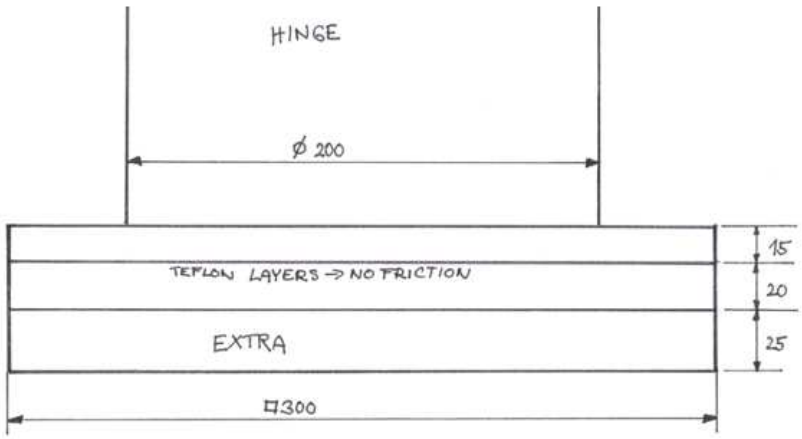

Figure 29: Composition of a loading plates for tests on slab S2, S3 and S8

Table 12: Composition of a loading plates for tests on slab S2, S3 and S8

S2T1	Without Extra plate
S3T1	Without Extra plate
S8T1	With Extra plate

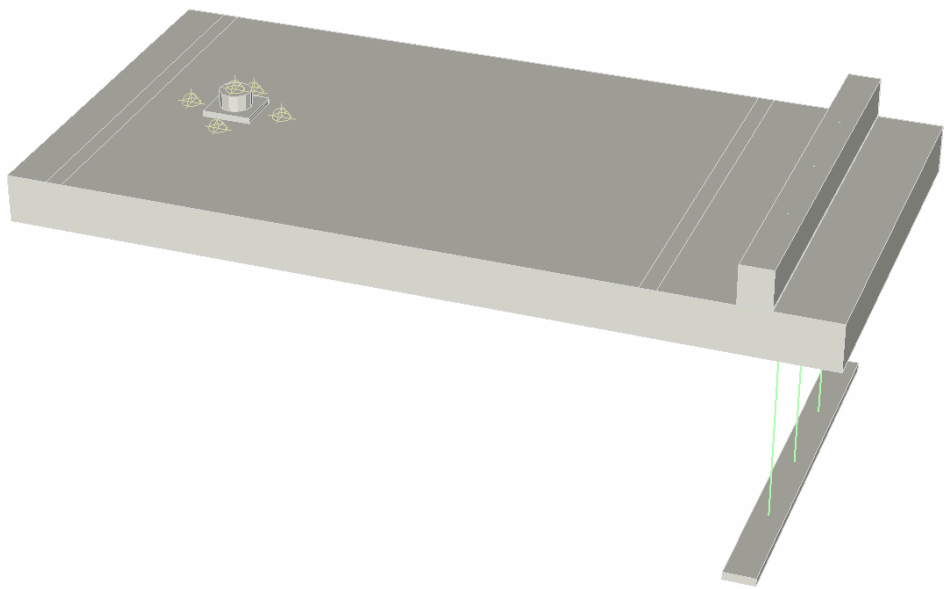

Figure 30: S2T1-013 model with two steel loading plates of the size 300x300 with teflon layer in between and loading jack of 200 mm diameter

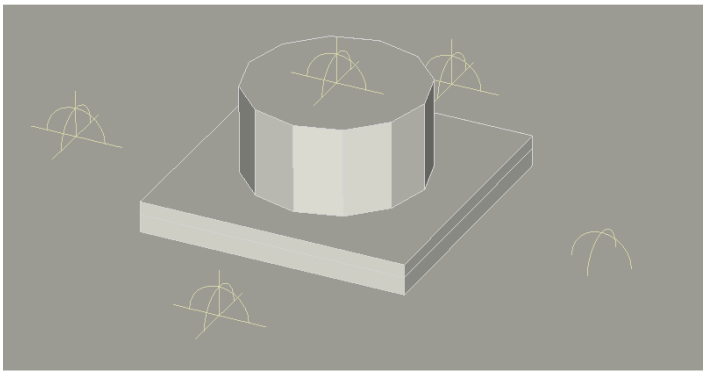

Figure 31: S2T1-013 model with two steel loading plates of the size 300x300 with teflon layer in between and loading jack of 200 mm diameter - detail

Table 13: Mechanical properties of the Teflon layer

Properties		**Value**	**Units**
Basic			
Normal stiffness	K_{nn}	2.000E+08*	MN/m^3
Tangential stiffness	K_{tt}	2.000E+08*	MN/m^3
Tensile strength	f_t	0.000E+00**	MPa
Cohesion	C	0.000E+00**	MPa
Friction coefficient	-	0.000E+00**	-
Miscellaneous			
Min. normal stiffness for num. purposes	$K_{nn,min}$	2.000E+05*	MN/m^3
Min. tangential stiffness for num. purposes	$K_{tt,min}$	2.000E+05*	MN/m^3

* default value; see reference CERVENKA, V., JENDELE, L., CERVENKA J. (2010)

** first assumption, simply changed to zero value

4.2. Results

The maximum load measured during experiment was 1374 kN. In the FEM analyses the maximum peak loads were in the range 682 – 942kN. In the percentage the difference of the results from the experiment and models is about 30 – 50 %. The best model with Teflon layer (presented in the Figure 32) had the peak load of 901 kN. This large difference in the peak loads of FEM models from the experimental results was not acceptable and therefore these models were not considered as finished yet. Further research would be advised.

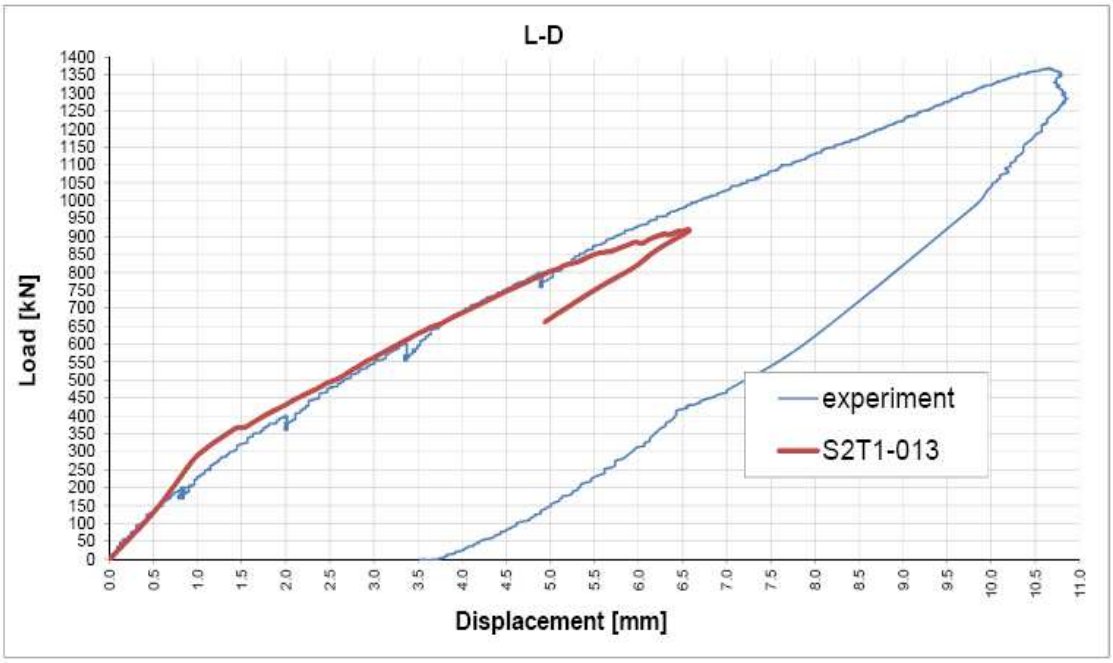

Figure 32: S2T1 load-displacement graph of the best model

4.3. Effective width

Although the FEM models for S2T1 were not finished, from the load-displacement graph it is obvious that FEM model results were very close to the experimental results until the load of 800 kN. The effective width was defined the same way as the effective width of the model S1T1. The effective widths for different loads are presented in Table 14.

The supports in the FEM model were modeled by the surface springs. The surface spring contained 52 nodes, which gave 26 nodes for each edge of the surface. For each node the value of the stress could be found and the effective width for different loads was determined. The crack visualization was filtered to the minimum crack width 0.0001 meters. In the model of S2T1 the first cracks of the size 0.0001 meters started to appear under the load of 368 kN and effective width at that load was 2.02 m (the width of the slab and length of the surface support was 2.5 meters).

Table 14: S2T1 effective width

S2T1-013			
Load [kN]	step	Cracks 0.0001 m	Effective Width [m]
55	24	No	2.4929
104	28	No	2.4664
146	31	No	2.4052
208	35	No	2.3489
256	38	No	2.3353
304	41	No	2.2861
353	44	No	2.1950
368	46	3	2.0256
395	48		1.8770
499	57		1.5635
601	65		1.4995
698	74		1.4781
803	84		1.4598
901	98		1.3806

5. S3T1

5.1. Model description

5.1.1. Concrete

S3 was casted from composition of concrete - Cast 2, and the test S3T1 was hold at the concrete age of 62 days. The concrete compressive strength was based on the cube test and the tensile strength on the tensile splitting test of the cube specimens casted from the same composition of the concrete and tested at the same age as corresponding concrete slabs (see reference LANTSOGHT, E.O.L., 2010).

In FEM model of S3T1 the same mechanical properties of the concrete as in the model of S1T1 were used (see Table 4), only the compressive and the tensile strengths were changed according the results on cube specimens. The concrete compressive strength for S3T1 was 52.10 MPa and the tensile strength was 4.22 MPa.

5.1.2. Felt

The test S1T1 was performed on the completely new felt placed between the steel beam support and the concrete slab. On this same felt the rest of tests on slab S1 and tests on slab S2 were hold. Each slab was tested in the six different locations. It was six tests performed on each slab. The slab S3 was tested on the same felt as slab S1 and S2. There were 12 test performed on the same felt before the test S3T1. Therefore the felt and plywood layer between the steel beam support and the concrete slab in the S3T1 model was defined according the properties of the *used* material. The second loading line of stress-strain diagram of the test 32 was used (see reference PROCHAZKOVA, Z., LANTSOGHT, E.O.L. (2011)). For the test 32 see the Figure 23 and for the stress-strain diagram used in the S3T1 FEM model see the Figure 33.

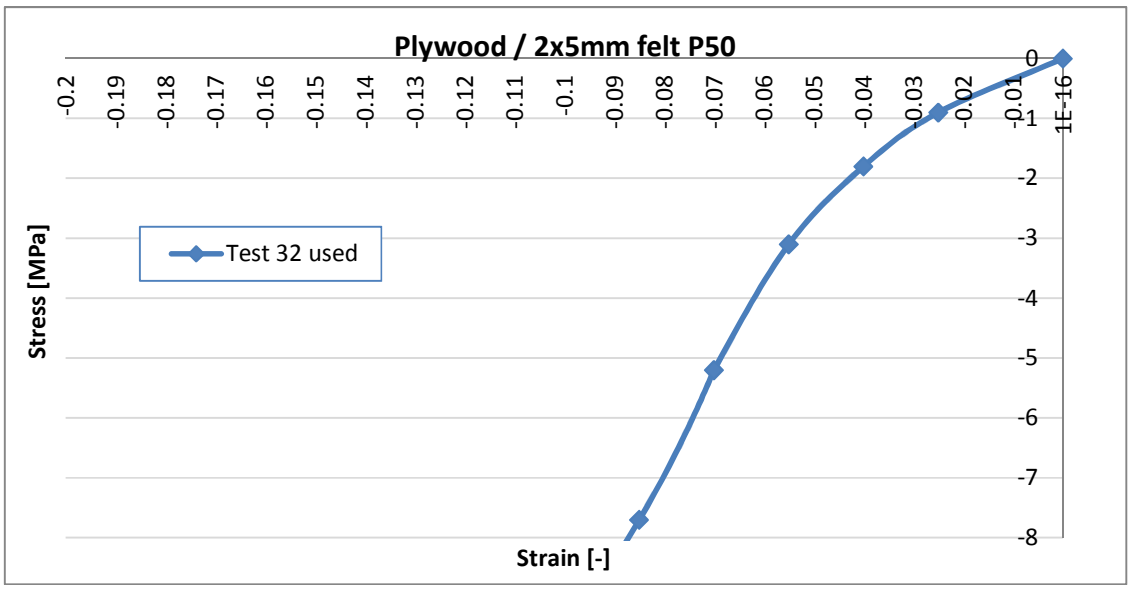

Figure 33: Stress-strain diagram of the surface spring properties of used material – nonlinear part only

5.1.3. Reinforcement

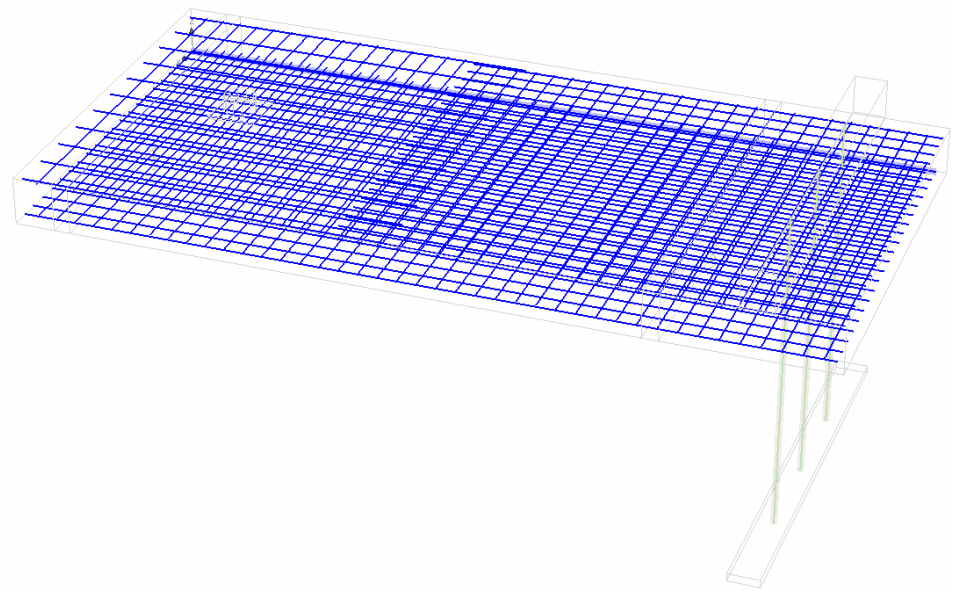

Figure 34: Model – reinforcement

The position of the longitudinal and transversal reinforcement of S3 and S8 could be seen in the Figure 34. The longitudinal reinforcement was of ϕ20 - 125mm (ρ_l = 0,996%) and the transversal reinforcement of ϕ10 - 125 mm (ρ_t = 0,132%). The modeling of the reinforcement overlaps and hooks was not necessary.

5.1.4. Loading plate

The loading plate's composition according the experiment for slabs S2, S3 and S8 are depicted in the Figure 29 and Table 12. For the slab S3 the loading plate composition consisted of two steel plates of thickness 15 and 20 mm with greasy Teflon layer (zero friction) in between steel plates and hinge for the loading jack of 200 mm diameter (see Figure 29).

The loading plate of the model S3T1-012 was modeled according the composition of the loading plate in the experiment and it was modeled the same way as in the model for S2T1 (Figure 30 and Figure 31).

The properties of the Teflon layer in the FEM models are summarized in the Table 13. The material 3D Interface was used and for the first models with the Teflon layer default values for the normal and tangential stiffness were left, only the friction coefficient and cohesion values were changed to zero. The better definition of the Teflon layer might be done to make FEM model closer to the reality but it would require more time investment, which was not available.

5.2. Results

The maximum load measured during experiment was 1371 kN. In the FEM analyses the maximum peak loads were around 900 kN. In the percentage the difference of the results from the experiment and models was about 34 %. The best model with the Teflon layer (presented in the Figure 32) had the peak load of 893 kN. This large difference in the peak loads of FEM models from the experimental results was not acceptable and therefore these models were not considered as finished yet. Further research would be advised.

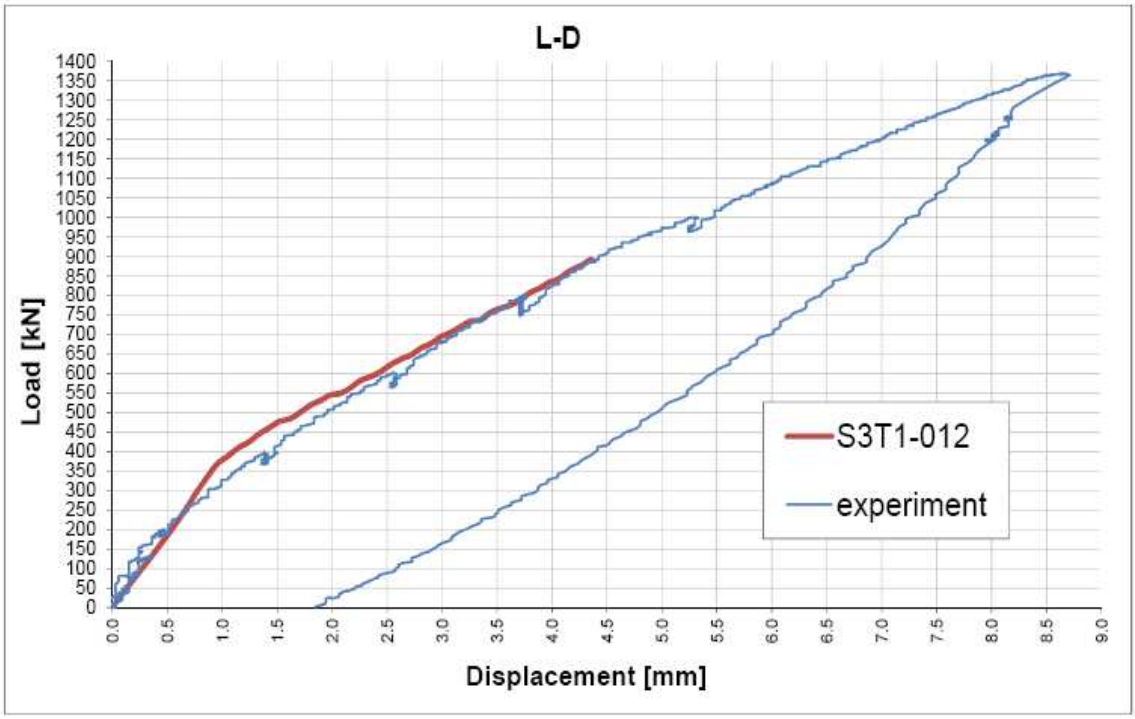

Figure 35: S3T1 load-displacement graph of the best model

5.3. Effective width

Although the FEM models for S3T1 were not finished (like models of S2T1), from the load-displacement graph it is obvious that the FEM model results were very close to the experimental results until the load of 900 kN. The effective width was defined the same way as the effective width of the model S1T1. The effective widths for different loads are presented in the Table 15.

The supports in the FEM model were modeled by surface springs. The surface spring contained 52 nodes, which gave 26 nodes for each edge of the surface. For each node the value of the stress could be found and the effective width for the different loads was determined. The crack visualization was filtered to the minimum crack width 0.0001 meters. In the model of S2T1 the first cracks of the size 0.0001 meters started to appear under the load of 460 kN and effective width at that load was 2.09 m (the width of the slab and length of the surface support was 2.5 meters).

Table 15: S3T1 effective width

S3T1-012			
Load [kN]	step	Cracks 0.0001 m	Effective Width [m]
42	16	No	2.4677
112	18	No	2.4111
147	19	No	2.3994
217	21	No	2.3411
257	22	No	2.2799
299	23	No	2.2757
370	25	No	2.2716
460	30	2 cracks	2.0943
477	31	4cracks	2.0655
592	40		1.7653
694	47		1.6112
787	55		1.4976
860	60		1.4591
893	70		1.4362

6. S8T1

6.1. Model description

6.1.1. Concrete

S8 was casted from the composition of the concrete - Cast 4, and the test S8T1 was hold at the concrete age of 48 days. The concrete compressive strength was based on the cube test and the tensile strength on the tensile splitting test of cube specimens casted from the same composition of the concrete and tested at same age as corresponding concrete slabs (see reference LANTSOGHT, E.O.L., 2010).

In the FEM model of S8T1 the same mechanical properties of the concrete as in the model of S1T1 were used (see Table 4), only the compressive and the tensile strengths were changed according the results on cube specimens. The concrete compressive strength for S3T1 was 77.02 MPa and the tensile strength was 6.00 MPa.

6.1.2. Reinforcement

The position of the longitudinal and transversal reinforcement of S3 and S8 could be seen in the Figure 34. The longitudinal reinforcement was of ϕ20 - 125mm (ρ_l = 0,996%) and the transversal reinforcement of ϕ10 - 125 mm (ρ_t = 0,132%). The modeling of the reinforcement overlaps and hooks was not necessary.

6.1.3. Loading plate

The loading plate's composition according the experiment for the slabs S2, S3 and S8 are depicted in the Figure 29 and the Table 12. For the slab S8 the loading plate composition consisted of two steel plates of thickness 15 and 20 mm with greasy Teflon layer (zero friction) in between steel plates, one extra steel plate of 25 mm thickness placed below the two thinner plates with the Teflon layer and the hinge for the loading jack of 200 mm diameter (see Figure 29).

The loading plate of the model S8T1-004 was modeled according the composition of the loading plate in the experiment and it was modeled the same way as in the model for S2T1 and S3T1 only the extra plate was added (Figure 36 and Figure 37).

The properties of the Teflon layer in the FEM models are summarized in Table 13. The material 3D Interface was used and for the first models with the Teflon layer default values for the normal and the tangential stiffness were left, only the friction coefficient and the cohesion values were changed to zero. The better definition of the Teflon layer might be done to make the FEM model closer to the reality but it would require more time investment, which was not available. In case of S8T1 there were also problems with felt properties which are described in a section below.

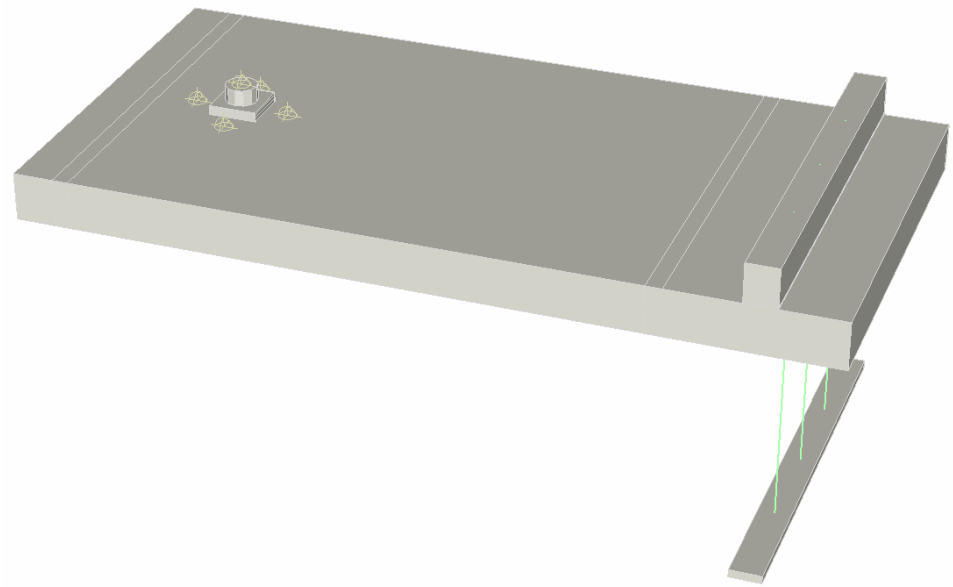

Figure 36: S8T1-004 model with three steel loading plates of the size 300x300 and hinge for the loading jack of 200 mm diameter

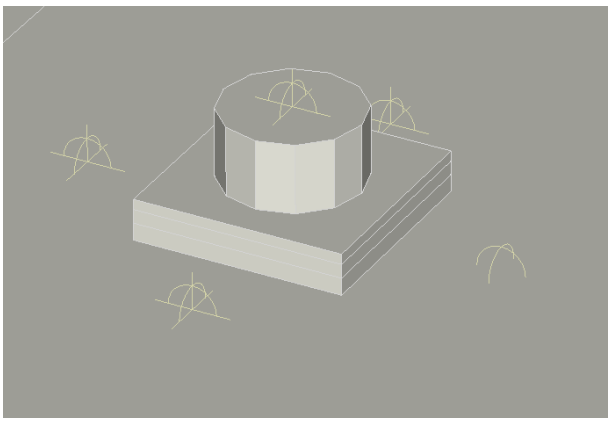

Figure 37: S8T1-004 model with three steel loading plates of the size 300x300 and hinge for the loading jack of 200 mm diameter - detail

6.1.4. Felt

From the modeling of test S1T1, S2T1 and S3T1 was found that the FEM models were very sensitive to the correct mechanical properties of the felt and plywood layer placed between the steel beam support and the concrete slab. It was also found that there was a difference between *new* and *used* felt material. Also there was found from the additional testing on the felt type P50 that there was a difference in the properties of the felt and plywood layer if the specimen was loaded for 24 hours under the constant load corresponding to the weight of the slab. The material faced some creep under that constant loading (see reference PROCHAZKOVA, Z., LANTSOGHT, E.O.L. (2011)).

For the composition of layers placed between the steel beam support and the concrete slab of the slab S8 the felt type N100 of thickness 15 mm was used. For that type of felt the additional test under the constant load was not made and therefore there were not available proper input data for the FEM model of the test S8T1.

The model S8T1-004 was made with the felt and plywood properties used in model of S1T1.

6.2. Results

The data of the mechanical properties of the felt type N100 and the plywood layer were not available and therefore the test S8T1 could not be properly modeled. Also the Teflon layer properties and the contact properties between the extra and the normal steel plates were not known and there was not found the correct way how to define them in the FEM model yet.

The model S8T1-004 is presented here as a reference model. The felt properties used in this model were properties of felt used in FEM model S1T1 and the loading plates were not correctly defined yet, but the load-displacement graph shows S8T1-004 results close to the experimental results. All calculations in the steps of this model were fully converged. Under the load of 503 kN the smaller prescribed displacement had to be used in order to have calculations fully converged. This usually represents a lot of cracking developing in the slab modeled in the FEM model. It would require too much time to refine the model to obtain cracking and therefore the calculation of the model S8T1-004 was stopped at this point. The effective width of this model is presented in the following section to see if the effective width changes with the same pattern as the effective widths of S1T1, S2T1 and S3T1.

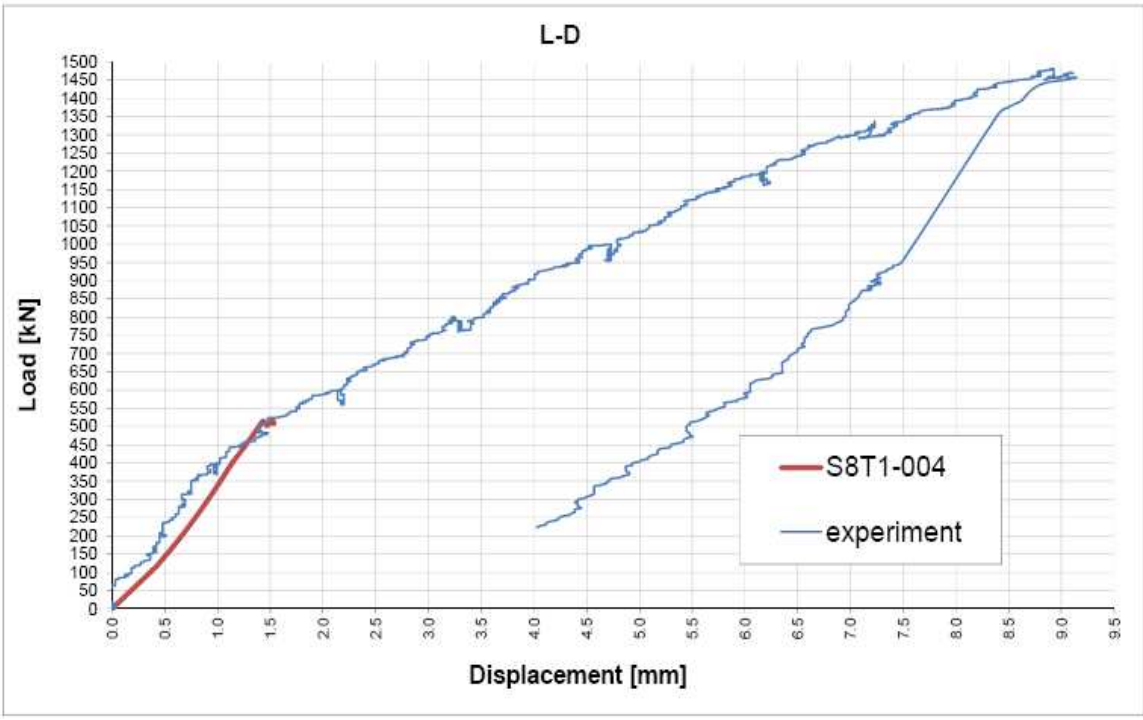

Figure 38: S8T1 load-displacement graph of the best model

6.3. Effective width

The model S8T1-004 is presented only as a reference model. The load-displacement graph of this model is close to the load-displacement graph of the experimental results. The effective widths for the different loads are presented in Table 15.

The supports in the FEM model were modeled by the surface springs. The surface spring contained 52 nodes, which gave 26 nodes for each edge of the surface. For each node the value of the stress could be found and the effective width for different loads was determined. The crack visualization was filtered to the minimum crack width 0.0001 meters. In the model of S2T1 the first cracks of the size 0.0001 meters might started to appear under the load of 503 kN and the effective width at that load was 2.29 m (the width of the slab and length of the surface support was 2.5 meters).

Table 16: S8T1 effective width

S8T1-004			
Load [kN]	step	Cracks 0.0001 m	Effective Width [m]
49	35	No	2.5
100	54	No	2.4970
139	67	No	2.4446
204	70	No	2.4043
260	73	No	2.3871
300	75	No	2.3676
362	78	No	2.3392
405	80	No	2.3381
458	83	No	2.3134
503	87	No	2.2924

7. Conclusions

Only the test S1T1 was completely modeled and the effective widths were found until the peak load. In the models of the other slabs the effective widths in the linear stage could be found and in the models of S2T1 and S3T1 also some effective widths after cracking were defined. From these result it might be possible to see that effective widths were reduced in similar manner with the increasing load.

The FEM analyses showed that the boundary conditions were very important for the behavior of the concrete slab. The boundary condition and especially the nonlinear properties of the felt had affected the crack pattern of the slab and the stiffness of the load-displacement diagram.

It was also found that the felt underwent some creep under the repeated loading. These changes could again affect the behavior of the reinforced concrete slab.

Further research on the felt properties and especially the felt type N100 would help to get improved FEM models.

Also the size and the thickness of the loading plate and the size of the hinge (through which load was applied) might have influence on the total capacity of the reinforced concrete slab.

8. Reference

LANTSOGHT, E.O.L., *Shear tests of Reinforced Concrete Slabs – Experimental data of Undamaged Slabs* (draft version November 5th,2010), TU Delft, The Netherlands, 334 pp

CERVENKA, V., JENDELE, L., CERVENKA, J., *Theory – ATENA Program Documentation* (March 22nd, 2010), Cervenka Consulting Ltd., Prague, The Czech Republic, 248 pp

PROCHAZKOVA, Z., LANTSOGHT, E.O.L., *Material properties – Felt and Reinforcement* For shear test of Reinforced Concrete Slabs (September 15th, 2011), Report nr. 25.5-11-11, TU Delft, The Netherlands, 28 pp